Targeted Disruption of the CD18 or ICAM-1 Gene Inhibits Choroidal Neovascularization

Eiji Sakurai,[1,2] *Hogara Taguchi,*[2,3] *Akshay Anand,*[1] *Balamurali K. Ambati,*[3,4] *Evangelos S. Gragoudas,*[3] *Joan W. Miller,*[3] *Anthony P. Adamis,*[3,5] *and Jayakrishna Ambati*[1,3]

Purpose. To investigate the role of the leukocyte adhesion molecules CD18 and intercellular adhesion molecule (ICAM)-1 in the development of choroidal neovascularization (CNV).

Methods. Laser photocoagulation was used to induce CNV in wild-type C57BL/6J mice and species-specific counterparts with targeted homozygous disruption of the CD18 or ICAM-1 gene. Expression of CD18 and ICAM-1 after laser injury was assessed by immunostaining. CNV responses were compared on the basis of en masse volumetric measurements obtained by confocal microscopy 2 weeks after laser injury and by determination of fluorescein angiographic leakage at 1, 2, and 4 weeks after laser injury.

Results. The site of laser injury showed upregulation of ICAM-1 and invasion by CD18-positive leukocytes within 1 day of laser injury. Significantly fewer lesions exhibited fluorescein leakage defined to be pathologically significant in CD18-deficient mice at weeks 1, 2, and 4 weeks and in ICAM-1–deficient mice at 1 and 4 weeks, compared with the control. There were a significantly greater number of lesions without fluorescein leakage in CD18-deficient mice than in the other two groups at all time points. The volume of CNV in CD18- and ICAM-1–deficient mice was significantly less than in wild type.

Conclusions. These data suggest a nonredundant role for leukocyte adhesion to vascular endothelium in the development of laser-induced choroidal neovascularization. (*Invest Ophthalmol Vis Sci.* 2003;44:2743–2749) DOI:10.1167/iovs.02-1246

From the [1]Department of Ophthalmology, University of Kentucky, Lexington, Kentucky; the [3]Department of Ophthalmology, Massachusetts Eye and Ear Infirmary, Harvard Medical School, Boston, Massachusetts; the [4]Department of Ophthalmology, Medical College of Georgia, Augusta, Georgia; and [5]Eyetech Research Center, Woburn, MA.

[2]Contributed equally to the work and therefore should be considered equivalent authors.

Supported by the American Ophthalmological Society Knapp Testimonial Fund (JA), a Foundation Fighting Blindness Career Development Award (JA), a Prevent Blindness America/Fight for Sight Grant-in-Aid (JA), a University of Kentucky Physician Scientist Award (JA), the Knights-Templar Eye Foundation (BKA), the Roberta Siegel Research Fund (APA), a Research to Prevent Blindness Senior Investigator Award (ESG), the Massachusetts Lions Eye Research Fund (APA, JWM), and the National Eye Institute (APA).

Submitted for publication December 5, 2002; revised January 16, 2003; accepted January 26, 2003.

Disclosure: **E. Sakurai**, None; **H. Taguchi**, None; **A. Anand**, None; **B.K. Ambati**, None; **E.S. Gragoudas**, None; **J.W. Miller**, None; **A.P. Adamis**, Eyetech Pharmaceuticals (E); **J. Ambati**, None

The publication costs of this article were defrayed in part by page charge payment. This article must therefore be marked "*advertisement*" in accordance with 18 U.S.C. §1734 solely to indicate this fact.

Corresponding author: Jayakrishna Ambati, Department of Ophthalmology, University of Kentucky, 740 S. Limestone Street, Lexington, KY 40536-0284; jamba2@uky.edu.

Age-related macular degeneration (AMD) is the leading cause of irreversible blindness among the elderly in most industrialized nations.[1] Yet, little is known about the molecular mechanisms of choroidal neovascularization (CNV), the angiogenic process responsible for most of the severe vision loss in patients with AMD.[2]

Leukocytes have been implicated in the pathogenesis of AMD, because their spatiotemporal distribution correlates with arborizing CNV in humans[3] and in animal models.[4] Macrophages are found in proximity to thinned and perforated areas of Bruch's membrane[5,6] and participate in the digestion of the outer collagenous zone of Bruch's membrane,[5] both of which facilitate the subretinal entry of CNV. There is growing evidence that leukocyte-mediated angiogenesis involves the interaction of cellular adhesion molecules and vascular endothelial growth factor (VEGF),[7,8] which itself is operative in CNV.[9–11] VEGF induces the expression of intercellular adhesion molecule (ICAM)-1 on tumor and retinal vascular endothelium and regulates leukocyte adhesion to endothelial cells.[12,13] ICAM-1 blockade decreases VEGF-induced leukostasis in the retina[13,14] and angiogenesis in the cornea.[8] These systems are intertwined: leukocytes, which possess receptors for and migrate in response to VEGF,[15] can also produce and release VEGF.[16]

The laser photocoagulation model of induced CNV captures many salient pathologic and molecular features of neovascular AMD. Therefore, we investigated the effects of ICAM-1 and its cognate receptor CD18 in a murine model of laser-induced CNV.

Methods

Animals

All animal experiments were in accordance with the guidelines of the University of Kentucky and Massachusetts Eye and Ear Infirmary Animal Care Committees and the ARVO Statement for the Use of Animals in Ophthalmic and Vision Research. CD18- (C57BL/6J-*Itgb2*^{tm1Bay}) and ICAM-1–deficient (C57BL/6J-*Icam1*^{tm1Bay}) mice, backcrossed onto the C57BL/6J background over 10 generations, were purchased from Jackson Laboratories (Bar Harbor, ME), as were wild-type C57BL/6J mice, which served as the control. Thus, these mice were expected to be more than 99.9% similar at all unlinked loci. Species specificity is important because genetic background determines susceptibility to neovascularization.[17] Only male mice between 4 and 6 weeks of age were used, to minimize variability, because age[18] and sex (Tanemura M, Miyamoto N, Mandai M, Honda Y, ARVO Abstract 530, 2001) can influence susceptibility to CNV. Genotypes were confirmed by PCR of genomic DNA extracted from tail snips. For all procedures, anesthesia was achieved by intramuscular injection of 50 mg/kg ketamine hydrochloride (Abbott, North Chicago, IL) and 10 mg/kg xylazine (Bayer, Shawnee Mission, KS), and pupils were dilated with topical 0.5% tropicamide (Alcon, Humacao, Puerto Rico).

Induction of CNV

Laser photocoagulation (630 nm, 400 mW, 0.05 second, 50 μm; model 920 Argon/Dye; Coherent Medical, Santa Clara, CA) was performed on

both eyes of each animal ($n = 10$ per group) by an operator masked to its genetic identity.[19] Four laser spots were applied in a peripapillary distribution in a standardized fashion, two to three disc diameters from the optic nerve, using a slit lamp delivery system and a coverslip as a contact lens. The morphologic end point of the laser injury was the appearance of a cavitation bubble, a sign thought to correlate with the disruption of Bruch's membrane.

Fluorescein Angiography

Fluorescein angiography was performed by an operator masked to the genetic identity of the animal, with a commercial camera and imaging system (TRC 50 VT camera and IMAGEnet 1.53 system; Topcon, Paramus, NJ), at 1, 2, and 4 weeks after laser photocoagulation. The photographs were captured with a 20-D lens in contact with the fundus camera lens, after intraperitoneal injection of 0.1 mL of 1% fluorescein sodium (Akorn, Decatur, IL).

Two masked retina specialists not involved in laser photocoagulation or angiography evaluated the fluorescein angiograms at a single sitting. Lesions were graded on an ordinal scale based on the spatial and temporal evolution of fluorescein leakage as follows: 0 (nonleaky): no leakage, faint hyperfluorescence, or mottled fluorescence without leakage; 1 (questionable leakage): hyperfluorescent lesion without progressive increase in size or intensity; 2A (leaky): hyperfluorescence increasing in intensity but not in size; no definite leakage; 2B (pathologically significant leakage): hyperfluorescence increasing in intensity and in size; definite leakage.

Volume of CNV

Two weeks after laser injury, eyes were enucleated and fixed with 4% paraformaldehyde for 30 minutes at 4°C. Eyecups obtained by removing anterior segments were washed three times in phosphate-buffered saline (PBS; Invitrogen-Life Technologies, Grand Island, NY), followed by dehydration and rehydration through a methanol series. After blocking was performed twice with buffer (PBS containing 1% bovine serum albumin [BSA; Sigma, St. Louis, MO]) and 0.5% Triton X-100 [Sigma]) for 30 minutes at room temperature (RT), eyecups were incubated overnight at 4°C with 0.5% fluorescein *Griffonia simplicifolia* lectin I (Vector Laboratories, Burlingame, CA), which binds to terminal β-D-galactose residues on the surface of endothelial cells and selectively labels the murine vasculature, diluted with PBS containing 0.2% BSA and 0.1% Triton X-100. After two washings with PBS containing 0.1% Triton X-100, the neurosensory retina was gently detached and severed from the optic nerve. Four relaxing radial incisions were made, and the remaining RPE-choroid-sclera complex was flatmounted (Immu-Mount Vectashield Mounting Medium; Vector) and coverslipped.

Flatmounts were examined with a scanning laser confocal microscope (TCS SP; Leica, Heidelberg, Germany). Vessels were visualized by exciting with blue argon laser wavelength (488 nm) and capturing emission between 515 and 545 nm. A 40× oil-immersion objective was used for all imaging studies. Horizontal optical sections (1-μm thickness step) were obtained from the surface of the RPE-choroid-sclera complex. The deepest focal plane in which the surrounding choroidal vascular network connecting to the lesion could be identified was judged to be the floor of the lesion. Any vessel in the laser-treated area and superficial to this reference plane was judged as CNV. Images of each section were digitally stored. The area of CNV-related fluorescence was measured by computerized image analysis with the microscope software (TCS SP; Leica). The summation of whole fluorescent area in each horizontal section was used as an index for the volume of CNV.

Immunostaining

Enucleated eyes were fixed (Histochoice MB; Amresco, Inc., Solon, OH) for 48 hours, and 7-μm paraffin sections were cut. Immunostaining was performed on deparaffinized sections preincubated with serum-free protein block (Dako, Carpinteria, CA) for 30 minutes at RT. Endogenous alkaline phosphatase activity was quenched with levamisole. Sections were then incubated for 1 hour at RT with rat anti-mouse CD18 (M18/2; Chemicon, Temecula, CA), rat anti-mouse ICAM-1 (KAT-1; R&D Systems, Minneapolis, MN), or rabbit anti-human von Willebrand Factor (A0082; Dako). Tissues were then incubated with diluted primary antibody (2–10 μg/mL) for 1 hour at RT. Diluted biotinylated secondary IgG (2–10 μg/mL) was applied for 30 minutes at RT. Signal amplification was obtained with a kit (Vectastain Indirect; Vector) followed by a streptavidin-biotin-alkaline phosphatase complex (ABC Kit; Vector). Color development was performed (Vector Red; Vector) and sections counterstained with hematoxylin. Specificity of staining was assessed by omitting the primary antibody.

Statistics

Fluorescein Angiography. Differences in incidence of grade-0 or -2B lesions between groups were analyzed by repeated-measures nested logistic regression. Because the probability development of CNV in each laser lesion is influenced by the group to which the lesion belongs, the mouse, the eye, and the laser spot, the nested design consisted of four measures (laser spots) per eye within two measures (eyes) per mouse within five measures (animals) per group. As the dependent variable (lesion grade) is ordinal with four levels, logistic regression considering both a between-subjects design (three groups, each with five animals) and a within-subjects design (two eyes and three time points) was performed. Because of the within-subjects part of the design, a repeated-measures analysis with the three factors (group, eye, time point) as main effects, and with two-way interactions was undertaken. Correlations between groups and lesion grades were analyzed by a multivariate permutation test. Two-tailed differences with a type I error not exceeding 0.05 were considered significant.

Volume of CNV. The mean lesion volumes were compared by using a linear mixed model with a split-plot, repeated-measures design. The whole-plot factor was the genetic group to which the animal belonged, and the split-plot factor was the eye. Statistical significance was determined at the 0.05 level. Post hoc comparison of means was constructed with a Bonferroni adjustment for multiple comparisons ($P < 0.017$).

Results

In wild-type C57BL/6J mice, numerous CD18- and ICAM-1–positive cells were concentrated at the site of the laser lesion as early as 1 day after injury and persisted up to 4 days (Fig. 1). These findings were restricted to the sites of injury and not generalized throughout the eye.

The volume of CNV in CD18-deficient mice was reduced by 67.0% ± 10.9% ($P < 0.0001$) and by 75.7% ± 8.6% ($P < 0.0001$) in ICAM-1–deficient mice, compared with wild-type C57BL/6J mice at 2 weeks after laser injury (Fig. 2). There was no statistically significant difference in CNV volume between the two knockout strains or between eyes within genetically identical groups. Both flatmounts and serial sections taken at 2 weeks after injury showed markedly smaller CNV membranes in CD18- and ICAM-1–deficient animals compared with those in wild types (Fig. 3).

At 1, 2, and 4 weeks after laser photocoagulation, pathologically significant leakage (grade-2B lesions) developed in most of the wild-type mice, but in significantly fewer CD18-deficient mice (Fig. 4). At weeks 1 and 4, significantly fewer lesions in the ICAM-1–deficient mice were grade-2B compared with wild-type animals, with a similar trend approaching significance at week 2. Fewer CD18-deficient mice ($P = 0.002$) and ICAM-1–deficient mice ($P = 0.028$) had three or more grade-2B lesions in each eye compared with the wild type (Fig. 5). At weeks 1 and 2, there was a significantly greater number of nonleaky (grade 0) lesions in the CD18-deficient mice than in the other two groups, with a similar trend approaching significance at

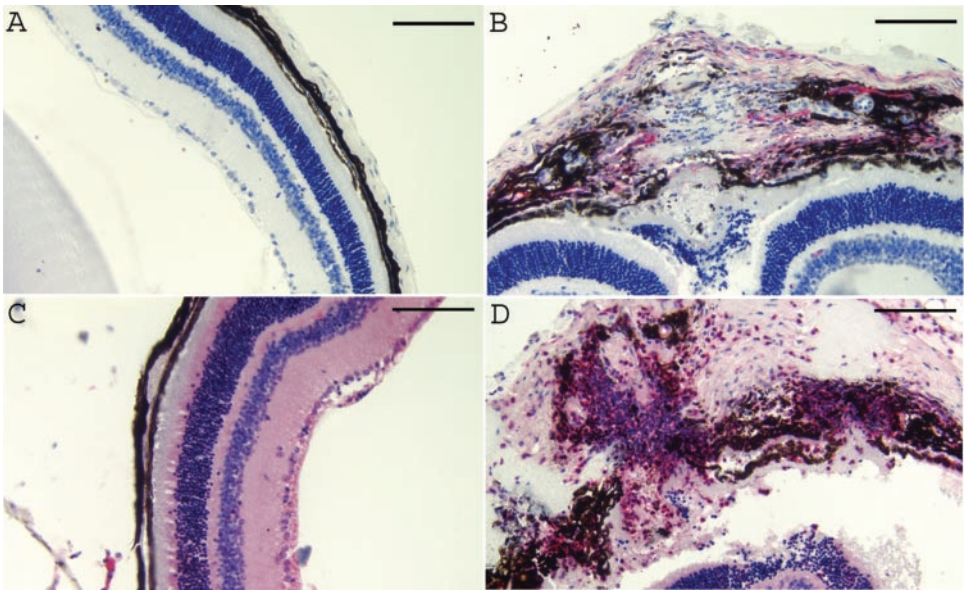

FIGURE 1. CD18- and ICAM-1–positive cells in CNV within 1 day of laser injury. (**A**, **C**) Unlasered areas showing normal neurosensory retina, retinal pigment epithelium (RPE), choroid, and sclera stained with red fluorescent dye and rat anti-mouse ICAM-1 (**A**) or rat anti-mouse CD18 (**C**). (**B**) Laser lesion (same section of eye as in (**A**) shows disruption and migration of RPE with high density of ICAM-1–expressing cells (presumed RPE and choroidal endothelial cells, stained with red fluorescent dye and rat anti-mouse ICAM-1), 1 day after injury. (**D**) Laser lesion (same section of eye as in (**C**) showing numerous CD18-positive cells (stained with red fluorescent dye and rat anti-mouse CD18) corresponding to surface of round *blue* cells (presumed leukocytes), 1 day after injury. Sections counterstained with hematoxylin (**A**, **B**) or hematoxylin and eosin (**C**, **D**). Scale bar, 100 μm. Original magnification, ×200.

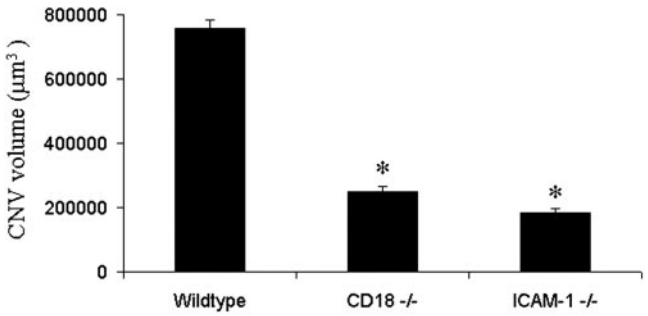

FIGURE 2. CNV volume was markedly diminished in CD18 and ICAM-1–deficient mice 2 weeks after laser injury. The volume per lesion (mean ± SEM) in $CD18^{-/-}$ (250,322.7 ± 15,071.9) and in $ICAM\text{-}1^{-/-}$ mice (184,744.8 ± 11,897.7) was significantly less than in wild-type animals (758,916.5 ± 26,077.6). $^{*}P < 0.0001$; $n = 5$ in all groups.

week 4 (Fig. 6). A trend toward a greater number of grade-0 lesions in the ICAM-1–deficient mice than in the control mice was observed. Odds ratios highlight the significant differences between proportions of grade-0 or -2B lesions between groups at all time points (Table 1). There were no significant intragroup differences in the proportion of grade-0 or -2B lesions at any time point in any of the three groups. No significant regression of CNV, as evaluated by fluorescein angiography, was observed within any group at the three time points. There was a high correlation between the group and the lesion grades ($r = 0.544$, $P < 0.001$).

DISCUSSION

In our study, CD18 or ICAM-1–deficient mice had smaller CNV membranes that also exhibit decreased fluorescein leakage than wild-type mice. This is consistent with the findings of ICAM-1 expression in the endothelial cells of CNV membranes in patients with AMD[20] (Nozaki M, Ozeki H, Ogura Y, ARVO Abstract 1229, 2001) and in laser-induced CNV in rats,[21] buttressing the growing body of evidence implicating leukocytes and leukocyte adhesion molecules in the initiation of angiogenesis.

The inhibition of CNV, although marked, was incomplete in both knockout groups, suggesting the presence of alternate mechanisms of angiogenesis. Nevertheless, the substantial inhibition of CNV in this model supports the hypothesis that

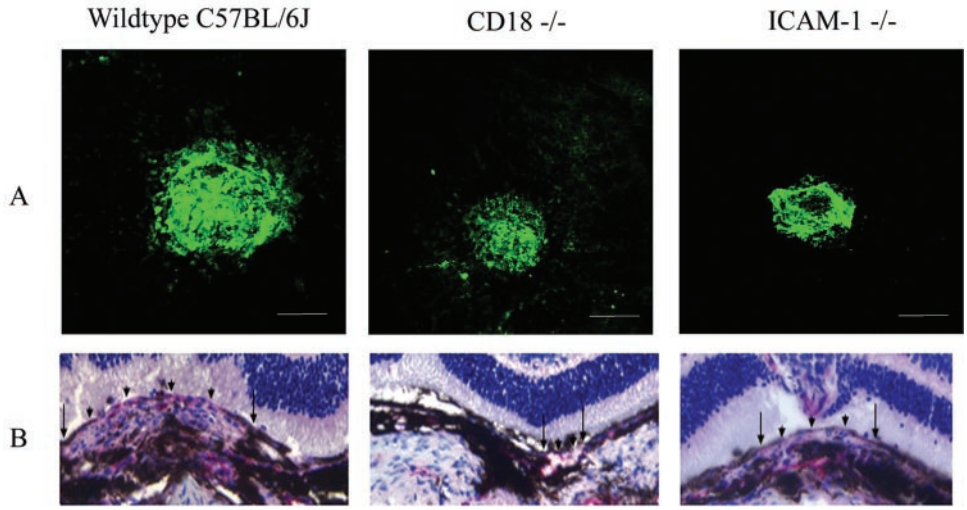

FIGURE 3. CNV size was markedly diminished in CD18- and ICAM-1–deficient mice 2 weeks after laser injury. (**A**) Stacked confocal images of fluorescein *Griffonia simplicifolia* lectin I-labeled tissue within laser scars show CNV membranes with a significantly smaller number in the mutant mice than in wild type. (**B**) Serial sections labeled with von Willebrand factor showed smaller CNV membranes, both in thickness and area. The section with the maximum diameter (*arrows*) for each CNV lesion, with thickness demonstrated by *arrowheads* along its surface, is shown. Scale bar, 100 μm.

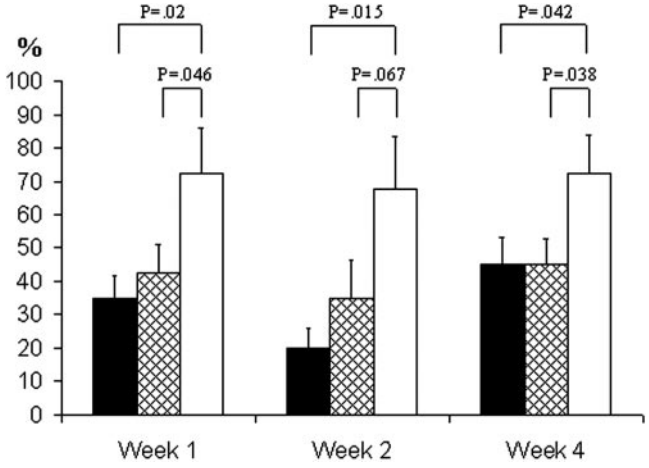

FIGURE 4. Significantly fewer grade-2B lesions occurred in CD18- and ICAM-1–deficient mice than in background C57BL/6J mice. Percentage of grade-2B lesions (mean ± SEM) in CD18-deficient (■), ICAM-1–deficient (▨), and wild-type (□) mice ($n = 5$ for all groups).

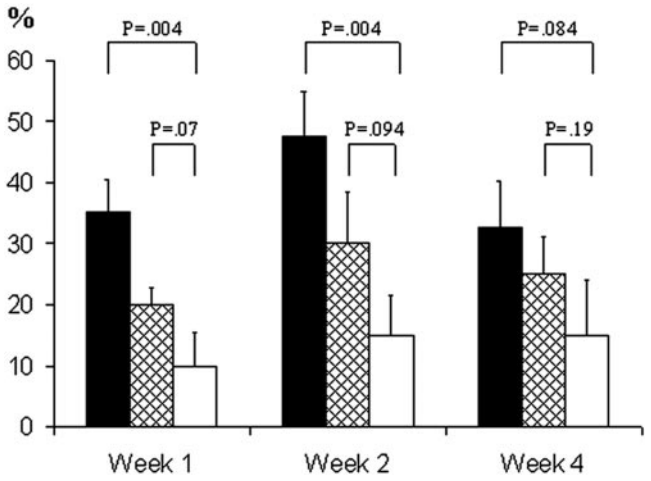

FIGURE 6. Significantly greater numbers of grade-0 lesions occurred in CD18-deficient mice compared with the control. Percentage of grade-0 lesions (mean ± SEM) in CD18-deficient (■), ICAM-1–deficient (▨), and wild-type (□) mice ($n = 5$ for all groups).

CD18 and ICAM-1 play a key role in initiating or at least facilitating CNV, particularly because cells expressing these markers are abundant in the site of CNV early after laser injury. Further, the extent of the requirement for CD18 and ICAM-1 in CNV may be more than demonstrated herein because genetic ablation is incomplete in these leaky knockouts.[22,23] In addition, the full contribution of leukocytes to CNV induction may not have been extracted in this paradigm because leukocyte adhesion sometimes can be CD18 independent.[24]

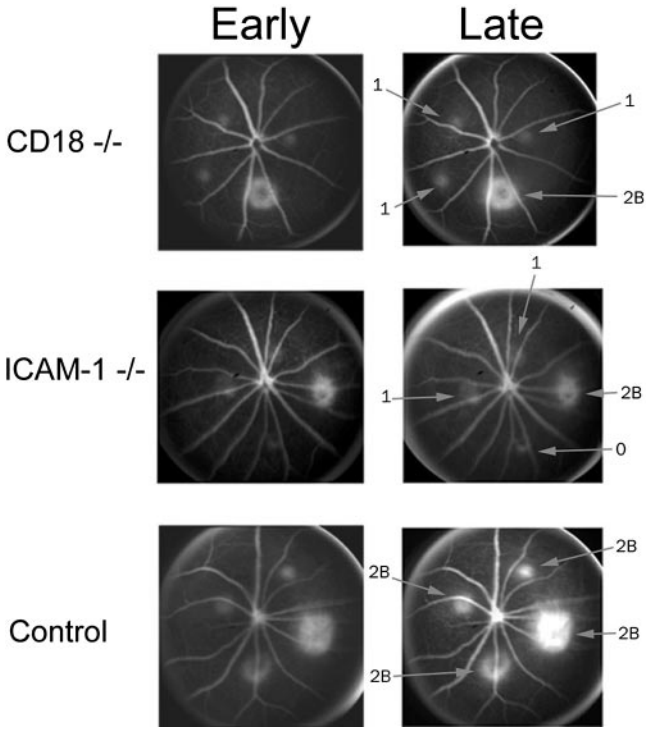

FIGURE 5. More control mice had three or more grade-2B lesions than did CD18- or ICAM-1–deficient mice. Representative early-phase (1–3 minutes) and late-phase (8–10 minutes) fluorescein angiograms of a $CD18^{-/-}$, $ICAM\text{-}1^{-/-}$, and wild-type C57BL/6J mouse. *Arrows*: lesion grades.

We found significantly greater inhibition of CNV-associated angiographic leakage in CD18-deficient than in ICAM-1–deficient mice, perhaps due to variations in the degree of hypomorphism in gene expression between the two groups, because these mutations are not completely null. Blockade of CD18 results in greater inhibition of leukocyte adhesion to RPE cells in response to inflammatory cytokines than blockade of ICAM-1.[25] This suggests that CD18 may recognize ligands other than ICAM-1, as appears to be the case in the accumulation of dendritic cells in the lung.[26] CD18 may bind to fibronectin,[27] which is found in the basement membrane of CNV in AMD.[5,28] Also, due to alternative RNA splicing, ICAM-1–deficient mice are not completely devoid of cell surface ICAM-1 expression[23] and contain normal levels of circulating soluble ICAM-1,[29] which can promote angiogenesis.[30]

A consensus has yet to evolve in quantifying experimental CNV. Both anatomic and functional metrics have been used. The former include measuring thickness and area on serial sections or volumes by confocal microscopy on RPE-choroidal flatmounts, aided by an endothelial cell marker. En masse volumetric measurements are less susceptible to nonorthogonality and loss/poor quality of sections than serial sectioning. Fluorescein angiography has been used to comment on the leakage of these lesions, presumably correlating with their activity due to incompetence of the immature vessels.

We used both anatomic and functional metrics of measuring CNV to reinforce the fidelity of our findings. Although both clinical[31,32] and experimental[33] CNV typically demonstrates fluorescein leakage, both types of CNV can be angiographically silent,[33–36] which correlates with envelopment by RPE.[37] In addition, fluorescein leakage correlates with visual acuity in patients with AMD,[38–40] and also permits longitudinal evaluation of the evolution of the laser lesions, unlike histopathological examination. Therefore, we defined grade-2B lesions, which have an angiographic and clinical appearance akin to classic CNV,[41] as pathologically significant. Notably, these are the type of lesion affected most by CD18 and ICAM-1 adhesion. Confocal microscopy disclosed the presence of CNV in grade-1, -2A, and -2B lesions but not in grade-0 lesions (Taguchi H, Kim RY, Razavi S, Connolly EJ, Gragoudas ES, Miller JW, ARVO Abstract 880, 2000). However, the hyperfluorescence of grade 1, and perhaps grade 2A, lesions may be due to transmission through RPE defects.

TABLE 1. Event Rates of Grade 0 and Grade 2B Lesions over 4-Week Period in CD18 or ICAM-1–Deficient Mice Compared with C57BL/6J Mice

	Grade 0 Lesions			Grade 2B Lesions		
Group	**Odds Ratio**	**95% CI**	***P***	**Odds Ratio**	**95% CI**	***P***
Control	1.00	—	—	1.00	—	—
$CD18^{-/-}$	5.29	1.7–16.4	0.004	0.11	0.02–0.58	0.01
$ICAM\text{-}1^{-/-}$	2.66	0.85–8.33	0.094	0.16	0.03–0.77	0.02

Although the laser-induced model of CNV may involve processes not relevant to AMD, it captures many of the important features of the human condition. Laser photocoagulation that disrupts Bruch's membrane can induce CNV in humans.[42] Both in experimental models and in AMD, newly formed vessels that are functionally incompetent[19,41,43] project into the subretinal space through defects in Bruch's membrane. Aggregation of leukocytes near arborizing neovascular tufts[3,4,44–46] is another shared feature of experimental and clinical CNV. Immunostaining has demonstrated the presence of VEGF and its receptors,[47,48] basic fibroblast growth factor,[49,50] transforming growth factor-β,[49,51] tumor necrosis factor-α,[45] Fas, and Fas-ligand[52,53] in cells composing the CNV membranes in both conditions.

We postulate that laser photocoagulation incites inflammation, leading to endothelial upregulation of ICAM-1, which binds to CD18, mediating firm leukocyte-endothelial adhesion and transmigration.[54] Laser photocoagulation leads to production of VEGF by RPE cells,[48] predominantly on the choroidal side.[55] In addition to stimulating proliferation of adjacent choroidal vascular endothelium, VEGF can upregulate ICAM-1 expression on endothelium.[12,13] Circulating leukocytes, which migrate in response to VEGF,[16] can then bind to this activated endothelium and to RPE.[25] Through their own release of VEGF,[16] leukocytes can amplify the locally produced VEGF response as they bind to the endothelium. Also leukocyte-derived cytokines can stimulate VEGF production in RPE cells[45] and choroidal fibroblasts.[56] Leukocytes can perpetuate their ingress by stimulating RPE cells to secrete the chemotaxins IL-8 and monocyte chemotactic protein-1 into the choroid in a polarized gradient[57,58] and to express ICAM-1 preferentially on the choroidal surface.[25] Leukocytes may also produce matrix metalloproteinases (MMPs) directly[59,60] or by releasing VEGF, which induces expression of MMP in endothelial cells.[61] These MMPs, which have been found in CNV in AMD,[62] can facilitate endothelial cell migration during angiogenesis.

In conclusion, the development of CNV is inhibited in mice deficient in the CD18 or ICAM-1 gene. Our observations suggest that CD18- and ICAM-1–mediated leukocyte adhesion are nonredundant events in the development of clinically apparent CNV, which is the principal cause of vision loss in AMD.[2] These findings may be relevant to neovascularization elsewhere in the body, where leukocytes and growing vessels are often found in proximity.[63] Because leukocytes are the principal purveyors of host defense, targeted methods of inhibiting adhesion molecules such as local drug delivery[64] would be desirable.

Acknowledgments

The authors thank Matthias Krause for critical review; Robinette King, Guojin Chen, and Edward Connolly for technical assistance; Ambati M. Rao and Delwood C. Collins for continued support; and Richard J. Kryscio, University of Kentucky Biostatistics Consulting Unit, and Wenjun Li, Massachusetts Eye and Ear Infirmary Biostatistics Center, for statistical analyses.

References

1. Klein R, Wang Q, Klein BE, Moss SE, Meuer SM. The relationship of age-related maculopathy, cataract, and glaucoma to visual acuity. *Invest Ophthalmol Vis Sci.* 1995;36:182–191.
2. Macular Photocoagulation Study Group. Argon laser photocoagulation for neovascular maculopathy: five-year results from randomized clinical trials. *Arch Ophthalmol.* 1991;109:1109–1114.
3. Grossniklaus HE, Cingle KA, Yoon YD, Ketkar N, L'Hernault N, Brown S. Correlation of histologic 2-dimensional reconstruction and confocal scanning laser microscopic imaging of choroidal neovascularization in eyes with age-related maculopathy. *Arch Ophthalmol.* 2000;118:625–629.
4. Nishimura T, Goodnight R, Prendergast RA, Ryan SJ. Activated macrophages in experimental subretinal neovascularization. *Ophthalmologica.* 1990;200:39–44.
5. van der Schaft TL, Mooy CM, de Bruijn WC, de Jong PT. Early stages of age-related macular degeneration: an immunofluorescence and electron microscopy study. *Br J Ophthalmol.* 1993;77:657–661.
6. Killingsworth MC, Sarks JP, Sarks SH. Macrophages related to Bruch's membrane in age-related macular degeneration. *Eye.* 1990;4:613–621.
7. Melder RJ, Koenig GC, Witwer BP, Safabakhsh N, Munn LL, Jain RK. During angiogenesis, vascular endothelial growth factor and basic fibroblast growth factor regulate natural killer cell adhesion to tumor endothelium. *Nat Med.* 1996;2:992–997.
8. Moromizato Y, Stechschulte S, Miyamoto K, et al. CD18 and ICAM-1-dependent corneal neovascularization and inflammation after limbal injury. *Am J Pathol.* 2000;157:1277–1281.
9. Spilsbury K, Garrett KL, Shen WY, Constable IJ, Rakoczy PE. Overexpression of vascular endothelial growth factor (VEGF) in the retinal pigment epithelium leads to the development of choroidal neovascularization. *Am J Pathol.* 2000;157:135–144.
10. Baffi J, Byrnes G, Chan CC, Csaky KG. Choroidal neovascularization in the rat induced by adenovirus mediated expression of vascular endothelial growth factor. *Invest Ophthalmol Vis Sci.* 2000;41:3582–3589.
11. Krzystolik MG, Afshari MA, Adamis AP, et al. Prevention of experimental choroidal neovascularization with intravitreal anti-vascular endothelial growth factor antibody fragment. *Arch Ophthalmol.* 2002;120:338–346.
12. Radisavljevic Z, Avraham H, Avraham S. Vascular endothelial growth factor up-regulates ICAM-1 expression via the phosphatidylinositol 3 OH-kinase/AKT/nitric oxide pathway and modulates migration of brain microvascular endothelial cells. *J Biol Chem.* 2000;275:20770–20774.
13. Miyamoto K, Khosrof S, Bursell SE, et al. Vascular endothelial growth factor (VEGF)-induced retinal vascular permeability is mediated by intercellular adhesion molecule-1 (ICAM-1). *Am J Pathol.* 2000;156:1733–1739.
14. Miyamoto K, Khosrof S, Bursell SE, et al. Prevention of leukostasis and vascular leakage in streptozotocin-induced diabetic retinopathy via intercellular adhesion molecule-1 inhibition. *Proc Natl Acad Sci USA.* 1999;96:10836–10841.
15. Clauss M, Weich H, Breier G, et al. The vascular endothelial growth factor receptor Flt-1 mediates biological activities. Implications for a functional role of placenta growth factor in monocyte activation and chemotaxis. *J Biol Chem.* 1996;271:17629–17634.

16. Harmey JH, Dimitriadis E, Kay E, Redmond HP, Bouchier-Hayes D. Regulation of macrophage production of vascular endothelial growth factor (VEGF) by hypoxia and transforming growth factor beta-1. *Ann Surg Oncol.* 1998;5:271–278.
17. Rohan RM, Fernandez A, Udagawa T, Yuan J, D'Amato RJ. Genetic heterogeneity of angiogenesis in mice. *FASEB J.* 2000;14:871–876.
18. Espinosa-Heidmann DG, Suner I, Hernandez EP, Frazier WD, Csaky KG, Cousins SW. Age as an independent risk factor for severity of experimental choroidal neovascularization. *Invest Ophthalmol Vis Sci.* 2002;43:1567–1573.
19. Tobe T, Ortega S, Luna JD, et al. Targeted disruption of the FGF2 gene does not prevent choroidal neovascularization in a murine model. *Am J Pathol.* 1998;153:1641–1646.
20. Heidenkummer HP, Kampik A. Surgical extraction of subretinal pseudotumors in age related macular degeneration. Clinical, morphologic and immunohistochemical results. *Ophthalmologe.* 1995;92:631–639.
21. Shen WY, Yu MJ, Barry CJ, Constable IJ, Rakoczy PE. Expression of cell adhesion molecules and vascular endothelial growth factor in experimental choroidal neovascularisation in the rat. *Br J Ophthalmol.* 1998;82:1063–1071.
22. Wilson RW, Ballantyne CM, Smith CW, et al. Gene targeting yields a CD18-mutant mouse for study of inflammation. *J Immunol.* 1993;151:1571–1578.
23. King PD, Sandberg ET, Selvakumar A, Fang P, Beaudet AL, Dupont B. Novel isoforms of murine intercellular adhesion molecule-1 generated by alternative RNA splicing. *J Immunol.* 1995;154:6080–6093.
24. Mizgerd JP, Kubo H, Kutkoski GJ, et al. Neutrophil emigration in the skin, lungs, and peritoneum: different requirements for CD11/CD18 revealed by CD18-deficient mice. *J Exp Med.* 1997;186:1357–1364.
25. Elner SG, Elner VM, Pavilack MA, et al. Modulation and function of intercellular adhesion molecule-1 (CD54) on human retinal pigment epithelial cells. *Lab Invest.* 1992;66:200–211.
26. Schneeberger EE, Vu Q, LeBlanc BW, Doerschuk CM. The accumulation of dendritic cells in the lung is impaired in CD18-/- but not in ICAM-1-/- mutant mice. *J Immunol.* 2000;164:2472–2478.
27. Rey-Ladino JA, Pyszniak AM, Takei F. Dominant-negative effect of the lymphocyte function-associated antigen-1 beta (CD18) cytoplasmic domain on leukocyte adhesion to ICAM-1 and fibronectin. *J Immunol.* 1998;160:3494–3501.
28. Das A, Puklin JE, Frank RN, Zhang NL. Ultrastructural immunocytochemistry of subretinal neovascular membranes in age-related macular degeneration. *Ophthalmology.* 1992;99:1368–1376.
29. van Den Engel NK, Heidenthal E, Vinke A, Kolb H, Martin S. Circulating forms of intercellular adhesion molecule (ICAM)-1 in mice lacking membranous ICAM-1. *Blood.* 2000;95:1350–1355.
30. Gho YS, Kleinman HK, Sosne G. Angiogenic activity of human soluble intercellular adhesion molecule-1. *Cancer Res.* 1999;59:5128–5132.
31. Teeters VW, Bird AC. A clinical study of the vascularity of senile disciform macular degeneration. *Am J Ophthalmol.* 1973;75:53–65.
32. Gass JD. Pathogenesis of disciform detachment of the neuroepithelium. *Am J Ophthalmol.* 1967;63:(suppl):1–139.
33. Ryan SJ. Subretinal neovascularization: natural history of an experimental model. *Arch Ophthalmol.* 1982;100:1804–1809.
34. Green WR, Key SN III. Senile macular degeneration: a histopathologic study. *Trans Am Ophthalmol Soc.* 1977;75:180–254.
35. Schneider S, Greven CM, Green WR. Photocoagulation of well-defined choroidal neovascularization in age-related macular degeneration: clinicopathologic correlation. *Retina.* 1998;18:242–250.
36. Miller H, Miller B, Ryan SJ. Correlation of choroidal subretinal neovascularization with fluorescein angiography. *Am J Ophthalmol.* 1985;99:263–271.
37. Miller H, Miller B, Ryan SJ. The role of retinal pigment epithelium in the involution of subretinal neovascularization. *Invest Ophthalmol Vis Sci.* 1986;27:1644–1652.
38. Miller JW, Schmidt-Erfurth U, Sickenberg M, et al. Photodynamic therapy with verteporfin for choroidal neovascularization caused by age-related macular degeneration: results of a single treatment in a phase 1 and 2 study. *Arch Ophthalmol.* 1999;117:1161–1173.
39. Treatment of Age Related Macular Degeneration with Photodynamic Therapy (TAP) Study Group. Photodynamic therapy of subfoveal choroidal neovascularization in age-related macular degeneration with verteporfin: one-year results of 2 randomized clinical trials—TAP report. *Arch Ophthalmol.* 1999;117:1329–1345.
40. Treatment of Age Related Macular Degeneration with Photodynamic Therapy (TAP) Study Group. Photodynamic therapy of subfoveal choroidal neovascularization in age-related macular degeneration with verteporfin: two-year results of 2 randomized clinical trials—TAP Report 2. *Arch Ophthalmol.* 2001;119:198–207.
41. Miller H, Miller B, Ishibashi T, Ryan SJ. Pathogenesis of laser-induced choroidal subretinal neovascularization. *Invest Ophthalmol Vis Sci.* 1990;31:899–908.
42. Francois J, De Laey JJ, Cambie E, Hanssens M, Victoria-Troncoso V. Neovascularization after argon laser photocoagulation of macular lesions. *Am J Ophthalmol.* 1975;79:206–210.
43. Sarks SH, Van Driel D, Maxwell L, Killingsworth M. Softening of drusen and subretinal neovascularization. *Trans Ophthalmol Soc UK.* 1980;100:414–422.
44. Penfold PL, Provis JM, Billson FA. Age-related macular degeneration: ultrastructural studies of the relationship of leucocytes to angiogenesis. *Graefes Arch Clin Exp Ophthalmol.* 1987;225:70–76.
45. Oh H, Takagi H, Takagi C, et al. The potential angiogenic role of macrophages in the formation of choroidal neovascular membranes. *Invest Ophthalmol Vis Sci.* 1999;40:1891–1898.
46. Pollack A, Korte GE, Heriot WJ, Henkind P. Ultrastructure of Bruch's membrane after krypton laser photocoagulation. II. Repair of Bruch's membrane and the role of macrophages. *Arch Ophthalmol.* 1986;104:1377–1382.
47. Otani A, Takagi H, Oh H, et al. Vascular endothelial growth factor family and receptor expression in human choroidal neovascular membranes. *Microvasc Res.* 2002;64:162–169.
48. Wada M, Ogata N, Otsuji T, Uyama M. Expression of vascular endothelial growth factor and its receptor (KDR/flk-1) mRNA in experimental choroidal neovascularization. *Curr Eye Res.* 1999;18:203–213.
49. Amin R, Puklin JE, Frank RN. Growth factor localization in choroidal neovascular membranes of age-related macular degeneration. *Invest Ophthalmol Vis Sci.* 1994;35:3178–3188.
50. Ogata N, Matsushima M, Takada Y, et al. Expression of basic fibroblast growth factor mRNA in developing choroidal neovascularization. *Curr Eye Res.* 1996;15:1008–1018.
51. Ogata N, Yamamoto C, Miyashiro M, Yamada H, Matsushima M, Uyama M. Expression of transforming growth factor-β mRNA in experimental choroidal neovascularization. *Curr Eye Res.* 1997;16:9–18.
52. Hinton DR, He S, Lopez PF. Apoptosis in surgically excised choroidal neovascular membranes in age-related macular degeneration. *Arch Ophthalmol.* 1998;116:203–209.
53. Kaplan HJ, Leibole MA, Tezel T, Ferguson TA. Fas ligand (CD95 ligand) controls angiogenesis beneath the retina. *Nat Med.* 1999;5:292–297.
54. Sligh JE Jr, Ballantyne CM, Rich SS, et al. Inflammatory and immune responses are impaired in mice deficient in intercellular adhesion molecule 1. *Proc Natl Acad Sci USA.* 1993;90:8529–8533.
55. Blaauwgeers HG, Holtkamp GM, Rutten H, et al. Polarized vascular endothelial growth factor secretion by human retinal pigment epithelium and localization of vascular endothelial growth factor receptors on the inner choriocapillaris. Evidence for a trophic paracrine relation. *Am J Pathol.* 1999;155:421–428.
56. Kvanta A. Expression and regulation of vascular endothelial growth factor in choroidal fibroblasts. *Curr Eye Res.* 1995;14:1015–1020.
57. Holtkamp GM, Van Rossem M, de Vos AF, Willekens B, Peek R, Kijlstra A. Polarized secretion of IL-6 and IL-8 by human

retinal pigment epithelial cells. *Clin Exp Immunol.* 1998;112: 34–43.

58. Holtkamp GM, De Vos AF, Peek R, Kijlsta A. Analysis of the secretion pattern of monocyte chemotactic protein-1 (MCP-1) and transforming growth factor-beta 2 (TGF-β2) by human retinal pigment epithelial cells. *Clin Exp Immunol.* 1999;118:35–40.
59. Peppin GJ, Weiss SJ. Activation of the endogenous metalloproteinase, gelatinase, by triggered human neutrophils. *Proc Natl Acad Sci USA.* 1986;83:4322–4326.
60. Banda MJ, Werb Z. Mouse macrophage elastase: purification and characterization as a metalloproteinase. *Biochem J.* 1981;193:589–605.
61. Lamoreaux WJ, Fitzgerald ME, Reiner A, Hasty KA, Charles ST. Vascular endothelial growth factor increases release of gelatinase A and decreases release of tissue inhibitor of metalloproteinases by microvascular endothelial cells in vitro. *Microvasc Res.* 1998;55: 29–42.
62. Steen B, Sejersen S, Berglin L, Seregard S, Kvanta A. Matrix metalloproteinases and metalloproteinase inhibitors in choroidal neovascular membranes. *Invest Ophthalmol Vis Sci.* 1998;39:2194–2200.
63. Knighton DR, Hunt TK, Scheuenstuhl H, Halliday BJ, Werb Z, Banda MJ. Oxygen tension regulates the expression of angiogenesis factor by macrophages. *Science.* 1983;221:1283–1285.
64. Ambati J, Gragoudas ES, Miller JW, et al. Transscleral delivery of bioactive protein to the choroid and retina. *Invest Ophthalmol Vis Sci.* 2000;41:1186–1191.